

# Reflectivity-Tunable Fiber Bragg Grating Reflectors

Ding-Wei Huang, Wen-Fung Liu, Cheng-Wen Wu, and C. C. Yang, *Senior Member, IEEE*

**Abstract**—We report a novel device that modulates the Bragg reflectivity of a fiber grating by exciting the transverse vibration of the fiber through an acoustic wave. The excitation of the transverse vibration, leading to fiber microbending, induces the coupling of the fiber core mode into cladding modes. This leads to the reduction of core-mode power and hence that of Bragg reflection. This mechanism provides us a means to control the reflectivity after a fiber Bragg grating is fabricated. The numerical results based on a simple micro-bending model agree well in trend with the experimental data.

**Index Terms**—Gratings, optical fiber devices, optical fiber filter.

**F**IBER Bragg gratings (FBG's) have been widely used in optical fiber communications [1], sensing [2] and lasers [3]. The most significant feature of an FBG is the relatively narrow bandwidth of its reflection spectrum. The reflection wavelength is determined by the grating period while the reflectivity is proportional to the depth of the index modulation. Usually, the index modulation can be as large as 0.001 with UV exposure of Ge-doped fiber and the reflectivity can be close to unity over the reflection band. Whatever the characteristics a FBG possesses, the reflectivity is fixed after it is fabricated. This property limits the application of an FBG.

In this letter, we present the experimental results of a reflectivity-tunable FBG reflector with acoustically excited transverse vibration of the fiber. With an appropriate excitation method, the transverse vibration can induce the coupling between the core mode and the cladding modes, thus the Bragg reflectivity can be changed. The Bragg reflectivity can be varied from its original value to almost zero. Hence, the device can serve as an acoustooptical fiber switch. Using an acoustic wave to control the behavior of the mode coupling in optical fiber has been discussed. Birks *et al.* used an acoustic wave to excite the transverse vibration of a four-port taper fiber coupler for shifting the coupling frequency [4]. Yun *et al.* used an acoustic wave to achieve tunable filtering in a two-mode fiber coupler [5]. Liu *et al.* used acoustic waves to excite the longitudinal vibration of an FBG for generating side bands of the reflection window [6]. The spectral location and intensity of the side bands were controlled by the acoustic frequency and intensity, respectively. Although this

mechanism can also be used for modulating reflectivity, it includes several disadvantages: 1) The original Bragg reflectivity needs to be close to unity for significant side-band generation; 2) The acoustic intensity needs to be quite strong for efficient operation; 3) the proximity of the side bands to the original reflection window makes the application difficult. On the contrary, with the excitation of transverse vibration of a fiber grating, we can directly modulate the Bragg reflectivity of a fiber grating after it is fabricated.

The system configurations are shown in Fig. 1(a) and (b). Either configuration includes an FBG, a piezoelectric transducer (PZT), a voltage source and a glass (or metal) horn. In Fig. 1(a), the thin end of a glass horn is spliced with the fiber grating. Its thick end, which is cut slant with an angle of  $5^\circ$ – $10^\circ$ , is glued to the PZT. In Fig. 1(b), The tip of an aluminum horn is transversely glued to the fiber. When we apply a high-voltage sinusoidal signal to the PZT, the induced acoustic wave propagates through the horn into the fiber with increasing amplitude along the horn. The acoustic wave excites the transverse vibration of the fiber (in the configuration of Fig. 1(a), the longitudinal vibration is also generated). To further increase the amplitude of the transverse vibration in the Bragg grating section, the fiber cladding was etched with hydrofluoric acid to form a tapered shape. The diameter of the fiber cladding was reduced to around  $40\ \mu\text{m}$  for sample 1 ( $30\ \mu\text{m}$  for sample 2). The length of the tapered region was about 16 mm for sample 1 (40 mm for sample 2). The grating length was 8 mm for sample 1 (20 mm for sample 2). Then, a broad-band signal, which was coupled into one end of the fiber was used to measure the change of the reflection spectrum. Fig. 2 shows the reflection spectra with different applied (peak-to-peak) voltage values at the PZT when sample 1 was used in the setup of Fig. 1(a). One can see that the peak reflectivity of the reflection spectrum has dropped from almost unity down to almost zero as the applied voltage increases. The frequency of the sinusoidal voltage signal was 730 kHz. From experiments, it was found that the acousto-modulated reflectivity change could occur only at certain acoustic frequencies, including 250, 730, and 1350 kHz.

Similar experiments were conducted with sample 2 in the setup of Fig. 1(b). In this case, both reflection and transmission spectra could be measured. Fig. 3(a) and (b) shows the reflection and transmission spectra with seven applied-voltage values at the PZT. The voltage frequency was fixed at 1.08 MHz. With zero voltage, the Bragg reflection peak is about unity. When the voltage increases to 74.2 V (p-p), the reflectivity drops to the level of noise. Meanwhile, one can see that the whole transmission spectrum in the measurement range drops with increasing voltage except for the Bragg reflection window. In the window, transmission intensity increases slightly first and then decreases with increasing voltage. However, the small transmission im-

Manuscript received August 23, 1999; revised October 13, 1999. This work was supported by the National Science Council, Republic of China, under Grant NSC 88-2215-E-002-012, Grant NSC 88-2112-M-002-004, and Grant NSC 88-2215-E-002-014.

D.-W. Huang and C. C. Yang are with the Department of Electrical Engineering and Graduate Institute of Electro-Optical Engineering, National Taiwan University, Taipei 106, Taiwan, R.O.C. (e-mail: ccy@cc.ee.ntu.edu.tw).

W.-F. Liu is with the Department of Electrical Engineering, Chung Cheng Institute of Technology, Tahsi, Taoyuan 335, Taiwan, R.O.C.

C.-W. Wu is with the Department of Applied Physics, Chung Cheng Institute of Technology, Tahsi, Taoyuan 335, Taiwan, R.O.C.

Publisher Item Identifier S 1041-1135(00)01115-0.

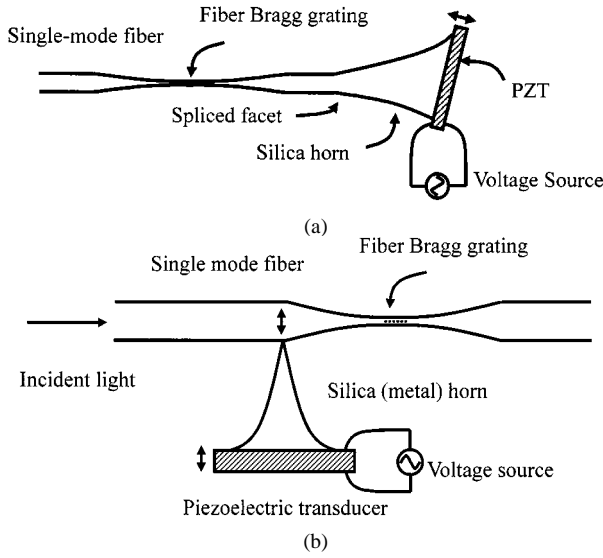


Fig. 1. Experimental setups of the device for exciting the transverse vibration of a fiber to control the reflectivity of an FBG. (a) Longitudinal excitation. (b) Transverse excitation.

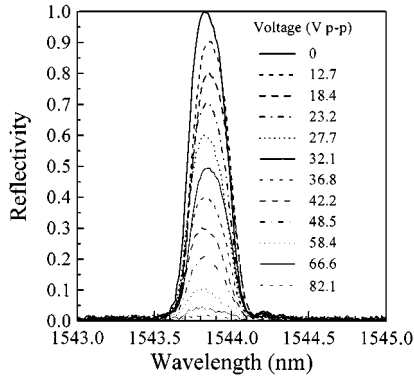


Fig. 2. Measured reflectivity spectra of an FBG based on the setup in Fig. 1(a) with different PZT driving voltages.

plies nothing conclusive but that most power coupled from the core mode into cladding modes becomes lost through radiation.

The observed phenomena can be explained with the mode coupling effect in the fiber grating. When the optical fiber vibrates transversely, signal power is coupled from the core mode into cladding modes. This phenomenon is similar to the situation that a fiber is under sinusoidal micro-bending, which provides the phase-matching mechanism [7]. In other words, the forward-propagating core mode, backward-propagating core mode, a group of forward-propagating cladding modes, and a group of backward-propagating cladding modes mutually couple. The counter-propagating core modes couple through the Bragg grating. The co-propagating core and cladding modes couple through fiber transverse vibration. The complete simulation of the device operation requires the solutions of at least four coupled differential equations. Because most of the cladding-mode power becomes lost through radiation, as shown in Fig. 3(b), we can use a simple model for demonstrating the variation of Bragg reflectivity. We assume that all the cladding-mode power radiates without any chance of coupling back to the core mode. In this situation, the out-coupled power from the forward-propagating core mode simply results in

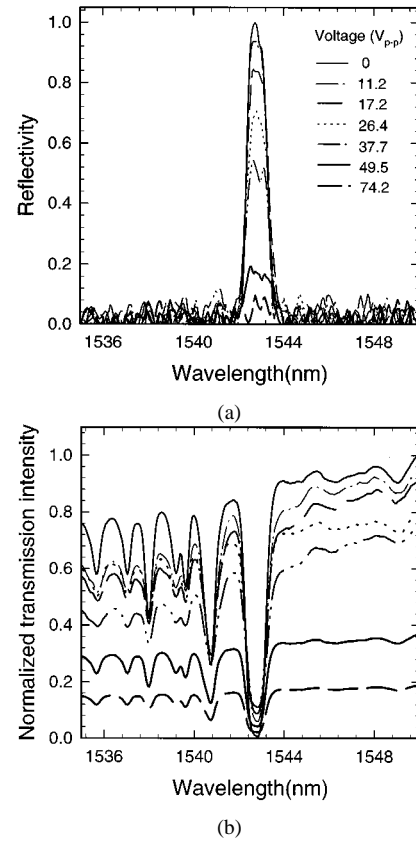


Fig. 3. (a) Measured reflectivity and (b) transmission spectra of an FBG based on the setup in Fig. 1(b) with different PZT driving voltages.

its attenuation along the fiber. In a further simplification, we assume that the coupling due to Bragg reflection results in a lumped wavelength-dependent reflection with an effective fiber length of mode coupling. Although such a model includes several approximations, it does provide us a picture for understanding the basic operation of the device. With the model, the attenuation constant of the forward-propagating core-mode due to the coupling into cladding-modes under transverse vibration, i.e.,  $\alpha_{tv}$ , can be calculated.

When a Bragg grating exists in the section of transverse vibration, the resultant reflectivity can be expressed as

$$R(\lambda) \approx |r(\lambda)|^2 \cdot \exp[-2\alpha_{tv}(\lambda) \cdot L_{tv}] \quad (1)$$

where  $r(\lambda)$  is the reflection coefficient of the Bragg grating and  $L_{tv}$  is the effective fiber length of mode coupling. The factor of two accounts for the round-trip of signal in the effective length of mode coupling. If the Bragg wavelength, i.e., the wavelength of the maximum  $r(\lambda)$ , coincides with a coupling peak, i.e., a maximum of  $\alpha_{tv}(\lambda)$ , the Bragg reflectivity decreases. This is the reason why we could observe significant reflectivity changes only at certain acoustic frequencies. Note that the decrease of the reflected power is proportional to the square of transverse vibration amplitude. In other words, the reduction of reflected power increases with the applied voltage for generating the acoustic wave. Hence, the Bragg reflectivity of the fiber grating can be controlled by the voltage.

Fig. 4 shows the calculated Bragg reflection spectra with various fiber vibration amplitudes. We assume that the effective

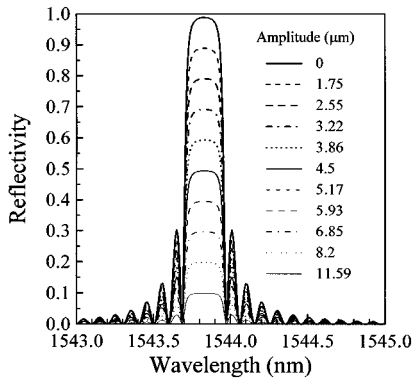


Fig. 4. Calculated reflectivity spectra of a uniform fiber Bragg grating with different transverse vibration amplitudes.

fiber length of mode coupling  $L_{TV}$  is 8 mm, the acoustic frequency is 730 kHz, and the sound speed in silica is 5400 m/s. A step-index profile is assumed with the core diameter at 5.25- $\mu\text{m}$  and the cladding diameter (after etching) at 40  $\mu\text{m}$ . The Bragg wavelength is 1540 nm. All the parameters were chosen to match the experimental conditions except that an ideal uniform FBG was assumed. It is expected that the fiber vibration amplitude is linearly proportional to the applied voltage. Therefore, the variation of vibration amplitude can be regarded as that of the applied voltage. Although based on a simple model, the numerical calculations agree well in trend with the experimental results in Fig. 2.

From Fig. 3(b), one notes that the transmitted power at certain wavelengths outside the Bragg reflection window was also attenuated through the induced micro-bending. This phenomenon results from the side lobes of core-cladding mode coupling. The wavelengths of attenuation and the attenuation levels depend on the cladding mode characteristics or the cladding thickness. Based on our calculations, these parameters can be adjusted for

particular applications by carefully controlling the etching conditions of fiber. Power loss may represent a drawback of the current device. However, it is speculated that by controlling the core-cladding coupling conditions, it is possible to have more power within the Bragg reflection window coupling back to the core mode in a region beyond the grating section. The back-coupling must occur before significant cladding mode radiation. Currently, we are evaluating the appropriate cladding thickness and etched length for optimum back-coupling. In summary, we have implemented a reflectivity-tunable fiber Bragg grating reflector with acoustic wave-excited transverse vibration of the fiber. With this technique, we could arbitrarily vary the Bragg reflectivity after a fiber grating was fabricated. The numerical results, based on a simple model of the coupling between the core-mode and cladding-modes, agreed well in trend with the experimental data.

#### REFERENCES

- [1] K. N. Park, Y. T. Lee, M. H. Kim, K. S. Lee, and Y. H. Won, "All-fiber drop-pass filters with fiber Bragg gratings," *IEEE Photon. Technol. Lett.*, vol. 10, pp. 555–557, 1998.
- [2] G. C. Lin, L. Wang, C. C. Yang, M. C. Shih, and T. J. Chuang, "Thermal performance of metal-clad fiber Bragg grating sensors," *IEEE Photon. Technol. Lett.*, vol. 10, pp. 406–408, 1998.
- [3] S. Yamashita and K. Hsu, "Single-frequency, single-polarization operation of tunable miniature erbium:ytterbium fiber Fabry-Perot lasers by use of self-injection locking," *Opt. Lett.*, vol. 23, pp. 1200–1202, 1998.
- [4] T. A. Birks, S. G. Farwell, P. St. J. Russell, and C. N. Pannell, "Four-port fiber frequency shifter with a null taper coupler," *Opt. Lett.*, vol. 19, pp. 1964–1966, 1994.
- [5] S. H. Yun, I. K. Hwang, and B. Y. Kim, "All-fiber tunable filter and laser based on two-mode fiber," *Opt. Lett.*, vol. 21, pp. 27–29, 1996.
- [6] W. F. Liu, P. St. J. Russell, and L. Dong, "100% efficient narrow-band acoustooptic tunable reflector using fiber Bragg grating," *J. Lightwave Technol.*, vol. 16, pp. 2006–2009, 1998.
- [7] V. Arya, K. A. Murphy, A. Wang, and R. O. Claus, "Microbend losses in singlemode optical fibers: Theoretical and experimental investigation," *J. Lightwave Technol.*, vol. 13, pp. 1998–2002, 1995.